

Solubilization properties of aqueous solutions of alkyltrimethylammonium halides toward a water-insoluble dye

A. Abe, T. Imae, and S. Ikeda

Department of Chemistry, Faculty of Science, Nagoya University, Chikusa, Nagoya, Japan

Abstract: The solubility of a water-insoluble dye, Sudan Red B, in aqueous sodium halide solutions of tetradecyl-, cetyl-, and stearyltrimethylammonium halides has been measured at different surfactant and salt concentrations, and the dependence of solubilization properties on alkyl chain length has been discussed with reference to the micelle size and shape. At low ionic strengths where only spherical micelles exist, the solubilization power of micellar surfactant slightly increases with increasing the ionic strength, but it sharply increases at high ionic strengths above the threshold value of sphere-rod transition. However, the solubilization power becomes independent of the ionic strength, if their rodlike micelles are sufficiently long. The solubilization capacity increases linearly with increasing the molecular weight, almost independent of counterion species, but the rodlike micelle has a higher solubilization capacity than the spherical micelle. The solubilization capacity is larger for a surfactant with longer alkyl chain, indicating that the dye is solubilized more readily in a larger hydrophobic core. The solubilized dye is situated in a rodlike micelle of alkyltrimethylammonium halides, on average, 4.5–7.5 nm apart from each other.

Key words: Solubility, solubilization power, Sudan Red B, alkyltrimethylammonium halide, rodlike micelle.

Introduction

The solubilization properties of aqueous solutions of surfactant are affected by various factors. The effect of salt concentration was first reported for the solubilization of transazobenzene in aqueous solutions of cetylpyridinium salts [1]. The solubilization power of micellar surfactant increased with the addition of electrolytes. The addition of KCl to aqueous solutions of potassium soap also increased the solubility of Orange OT [2, 3] and ethylbenzene [4]. The solubility of phenothiazine in aqueous solution of sodium dodecyl sulfate changed with the addition of 0.15 M NaCl [5]. The addition of salt to aqueous solutions of ionic surfactant increases the solubilization of nonpolar solubilizes in the hydrophobic inner core of a micelle [6].

The solubilization in micellar solution is also affected by the counterion species [5–9]. While the solubilization of dimethylaminoazobenzene is not very different for sodium and potassium soaps [7], the solubilization power of aqueous solutions of dodecyl-2-hydro-

xyethylammonium salts toward some organic solubilizes varies of the order $\text{NO}_3^- \approx \text{I}^- > \text{Br}^- > \text{Cl}^-$ [9]. The solubility of phenothiazine in aqueous solution of manganese or zinc dodecyl sulfate is larger than that of sodium dodecyl sulfate [5].

The effect of structure of the surfactant on its solubilization behavior has been investigated by various workers [2, 3, 7, 10, 11]. The dependence on the chain length of poly(oxyethylene) group was reported for the solubilization properties of micelles of sodium dodecyl poly(oxyethylene) sulfate and poly(oxyethylene) dodecyl ether toward Yellow OB [10]. An increase in alkyl chain length of surfactant generally enhances its solubilization property. The solubility of Orange OT or dimethylaminoazobenzene in aqueous solutions of potassium soaps with C_8 to C_{14} illustrates this effect [2, 3, 7]. The solubilization capacity of a micelle of alkylpyridinium chloride in 0.5 M NaCl solutions for some solubilizes also increased with an increase in the alkyl chain length from C_{10} to C_{16} [11].

We have recently investigated the solubilization of a water-insoluble azo-dye, Sudan Red B, in aqueous NaCl and NaBr



Sudan red B

solutions of dodecyltrimethylammonium chloride (DTAC) and bromide (DTAB), respectively [12], and found that the solubilization power of DTAB increased with NaBr concentration, gradually for spherical micelles and sharply for rodlike micelles, while that of DTAC was almost constant for the NaCl concentrations from 0 to 4 M. The solubilization capacity of spherical micelles of dodecyltrimethylammonium ions (DTA^+) was nearly independent of counterion species, either chloride or bromide.

In this work we measure the solubility of Sudan Red B in aqueous NaCl and NaBr solutions of tetradecyl-, cetyl-, and stearyltrimethylammonium chlorides (TTAC, CTAC, STAC) and bromides (TTAB, CTAB, STAB), respectively, and discuss their solubilization properties in relation to the alkyl chain length of alkyltrimethylammonium halide as well as to the effects of salt concentration and counterion species.

According to our light scattering measurements [13–15], tetradecyl- and cetyltrimethylammonium halides form spherical micelles in aqueous solutions above the critical micelle concentration and the size of spherical micelles gradually increases with addition of sodium halides. Rodlike micelles are formed at salt concentrations above certain threshold values. The size or contour length of rodlike micelles sharply increases with an increase in sodium halide concentration.

Experimental

Materials

DTAC, DTAB, TTAC, TTAB and CTAB are the same samples as previously recrystallized and used [12–14]. CTAC and STAC were purchased from Tokyo Kasei Kogyo Co., Ltd., Tokyo, recrystallized three times from an ethanol-acetone mixture, and dried in vacuo at 60°C for 8 h. STAB was kindly presented to us by Dr. Kenichi Hattori of Kao Corporation, Tokyo, recrystallized twice

from an ethanol-acetone mixture and once from an acetone-ethyl acetate mixture, and dried in vacuo at 60°C for 8 h.

Sudan Red B (Merck Sudan III, color index number 26110) is the same sample as previously used [12]. It was kindly supplied to us by Prof. Eiji Ohnishi and used without further purification. Absorption spectra of Sudan Red B in a water-ethanol (1:1) mixture have a main band at 506–507 nm and a shoulder around 530 nm.

Commercial NaCl and NaBr were ignited for 1 h. Ethanol is a spectrograde reagent from Nakarai Chemicals, Ltd., Kyoto. Water was redistilled from alkaline KMnO_4 .

Gas chromatography

Gas chromatographic analysis of surfactants was carried out on a Shimadzu Gas Chromatograph GC-5A, with a 1.5 m column. When Tenax GC was used as a column packing agent, some contaminant peaks were detected besides a sample peak in all examinations, common to surfactant species. Thus the source of the contaminants is attributable to the column packing agent. On a Silicone OV-1 column, no extra peaks coming from the column packing agent were detected, but two peaks from a surfactant were observed, of which the faster one is stronger and the slower one is weaker.

The gas chromatograms of the alkyltrimethylammonium halides on a Versamid 900 column are shown in Figure 1. A sample dissolved in ethanol was injected into the thermal reservoir at 300°C and passed through the column at 180°C under the flow of N_2 gas at 0.6 kg/cm². There was a single asymmetric peak from the surfactant, besides ethanol, on each chromatogram, but no appreciable peak of homologs was observed, thus indicating that surfactants are pure. For STAB, a small peak appeared at the position near the peak of DTAB or the second peak of ethanol: this peak is identified with the second peak of ethanol, since it remains weak even when the peak of STAB becomes stronger for a more concentrated STAB solution. As plotted in Figure 2(a), the flow time, l (arbitrary unit), for surfactants can be related to the number of carbon atoms of their alkyl chain, n_c , by

$$\log l = 0.14_2 n_c - 1.7_5, \quad (1)$$

independent of the counter-ion species, either chloride or bromide.

Solubilization measurements

Measurements of absorption spectra were carried out on a Hitachi 228 double beam spectrophotometer equipped with a Hitachi MB-6390 personal computer, at room temperature (25 ± 1°C). Quartz cells with path length of 5 and 10 mm were used.

Crystalline Sudan Red B was added to an aqueous salt solution of surfactant, and the suspension was shaken for 2 days at 25 ± 0.2°C, unless otherwise stated, in a water bath incubator BT-22, Yamato Scientific Co., Inc. The solubilization equilibrium in the suspension was attained within 2 days. Then the excess insoluble dye was filtered off with a Millipore filter FGLP 01300 having a pore size of 0.2 μm. An aliquot of the first filtrate was discarded in order to minimize the error from the adsorption of dye on the filter. After the remaining filtrate was diluted with an equal volume of ethanol, the absorption spectrum of the mixed solution was measured.

The 4.0 M NaCl solution of TTAB, the aqueous solutions of CTAB with NaBr concentrations more than 0.01 M, and the aque-

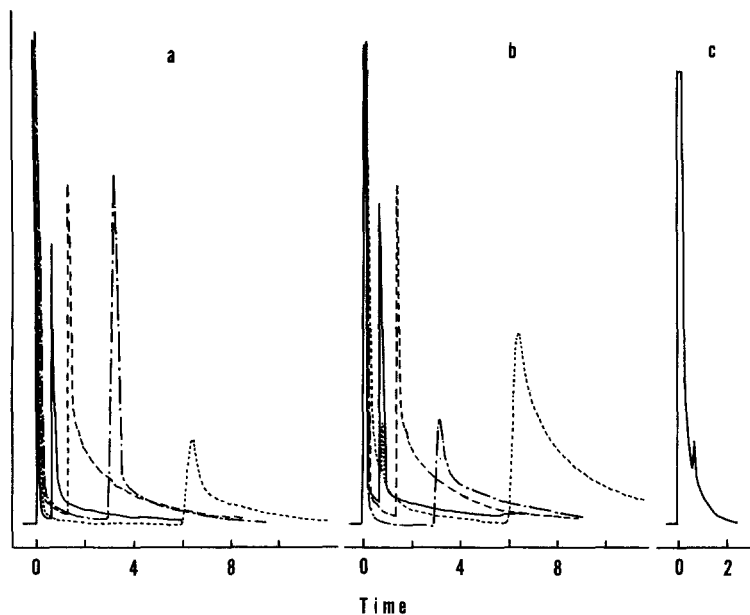
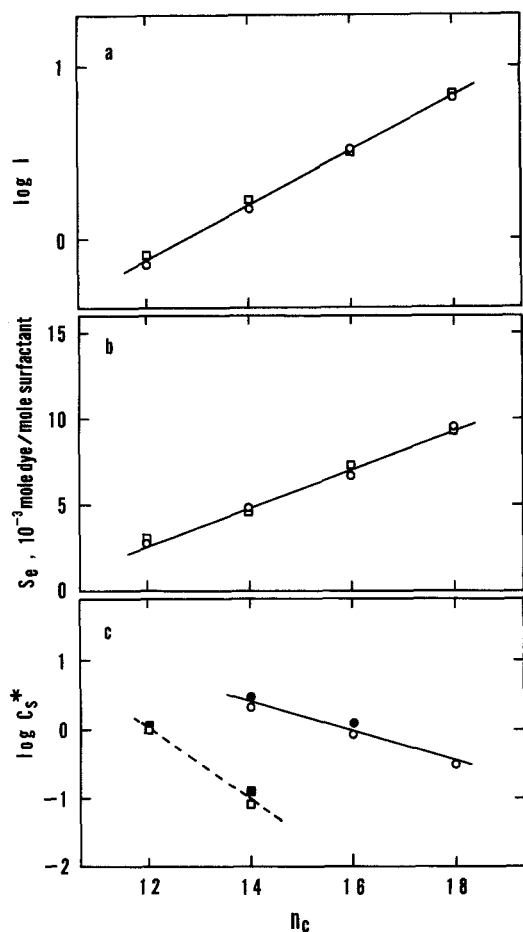


Fig. 1. Gas chromatogram of alkyltrimethylammonium halides on a Versamid 900 column. a) (—) DTAC; (---) TTAC; (---) CTAC; (---) STAC. b) (—) DTAB; (---) TTAB; (---) CTAB; (---) STAB. c) (—)



ous solutions of STAC above 1.0 M NaCl yielded precipitates at 25 °C, and STAB was not soluble even in water at 25 °C. The experiments for STAC in 1.0 M NaCl and for STAB in water were carried out at $35 \pm 0.2^\circ\text{C}$.

The molar concentration of the azo-dye solubilized in aqueous salt solution of surfactant, S (M), was determined by optical density measurement, as described elsewhere [12].

In the solubilization experiments for 2.0–4.0 M NaCl solutions of CTAC, the mixed solutions with high surfactant concentrations yielded precipitates when an equal volume of ethanol was added to the filtrate. The mixed solutions were then further diluted by the same volume of a water-ethanol (1:1) mixture, in order to obtain the clear solution for optical density measurement.

Results

Figure 3 shows the molar concentration of Sudan Red B, S (M), solubilized in aqueous NaCl solutions of TTAC against the molar concentration of surfactant, C (M). The solubility of the dye in aqueous solutions of TTAC without NaCl increases above the surfactant concentration of 4.62×10^{-3} M, which can be identi-

Fig. 2. a) Flow time on gas chromatogram, b) solubilization power of a spherical micelle in water, and c) threshold salt concentration of sphere-rod transition against the number n_c of carbon atoms of alkyl chain. (a), (b), (c): (○), (●) chloride derivatives; (□), (■) bromide derivatives. (c): (○) (□) by solubilization method; (●), (■) by light scattering method

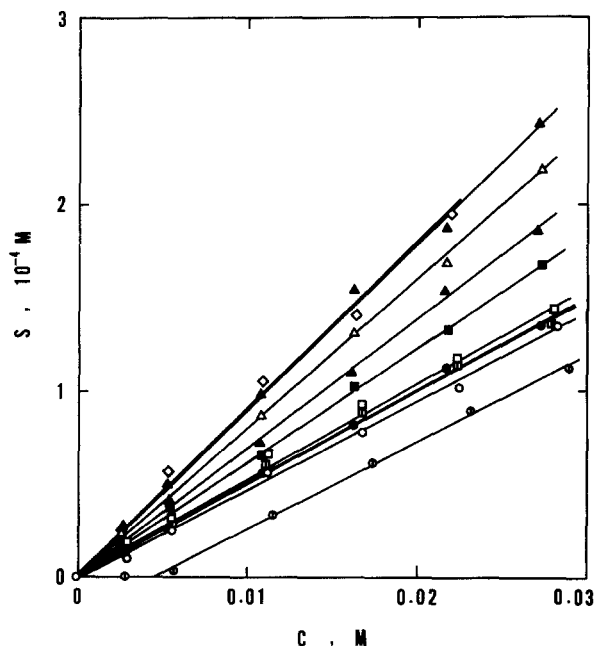


Fig. 3. Solubility of Sudan Red B in aqueous NaCl solutions of TTAC as a function of molar concentration of surfactant at 25 °C. NaCl concentration (M): (○) 0; (○) 0.01; (●) 0.50; (▨) 1.00; (□) 2.00; (■) 2.51; (△) 3.03; (△) 3.50; (▲) 4.00; (◇) 4.54

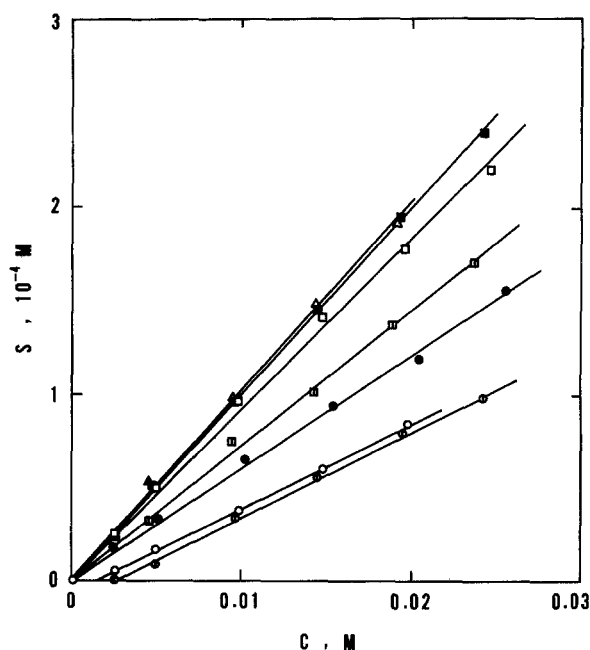


Fig. 4. Solubility of Sudan Red B in aqueous NaBr solutions of TTAB as a function of molar concentration of surfactant at 25 °C. NaBr concentration (M): (○) 0; (○) 0.007; (●) 0.13; (▨) 0.25; (□) 0.50; (■) 0.99; (△) 2.03

fied with the critical micelle concentration, C_o (M). This value is slightly lower than that measured by light scattering, 8.22×10^{-3} M [14]. The critical micelle concentration is very low for aqueous solutions of TTAC with NaCl concentration above 0.01 M.

The solubility of Sudan Red B in aqueous NaBr solutions of TTAB is plotted against the molar concentration of surfactant in Figure 4. The critical micelle concentration was obtained as 2.47×10^{-3} M in water, as 1.57×10^{-3} M in 0.007 M NaBr, and below 10^{-4} M for NaBr concentrations beyond 0.055 M. The critical micelle concentration values are close to 3.86×10^{-3} M in water and 1.78×10^{-3} M in 0.01 M NaBr which were determined by light scattering [14].

The solubilization behavior of CTAC in 0–4.0 M NaCl, CTAB in water and in 0.01 M NaBr, STAC in 0–1.0 M NaCl, and STAB in water toward the dye is similar to that of TTAC and TTAB. The critical micelle concentration was obtained as 0.98×10^{-3} M for CTAC in water and as 0.82×10^{-3} M for CTAB in water. The latter value is comparable with 0.9×10^{-3} M at 35 °C observed in our light scattering measurement [13]. The critical micelle concentration values for micelles in water observed from solubilization meas-

urements are listed in Table 1, together with those for DTAC and DTAB micelles [12].

The solubility of dye increases linearly with increasing micelle concentration, $C - C_o$ (M). The slope of the straight line at a given salt concentration represents moles of dye solubilized per mole of micellar surfac-

Table 1. The critical micelle concentration of surfactants and the solubilization parameters of their spherical micelles in water at 25 °C

	C_o (10^{-3} M)	S_e ($\frac{10^{-3} \text{ mole dye}}{\text{mole surfactant}}$)	Σ ($\frac{\text{mole dye}}{\text{mole micelle}}$)
DTAC ^a)	18.8	2.81	0.123
DTAB ^a)	14.7	2.85	0.151
TTAC	4.62	4.70	0.268
TTAB	2.47	4.58	0.324
CTAC	0.98	6.61	0.542
CTAB	0.82	7.25	0.660
STAC	~ 0.09	9.29	
STAB	—	9.24 ^b)	

^a) Reference [12]; b) at 35 °C

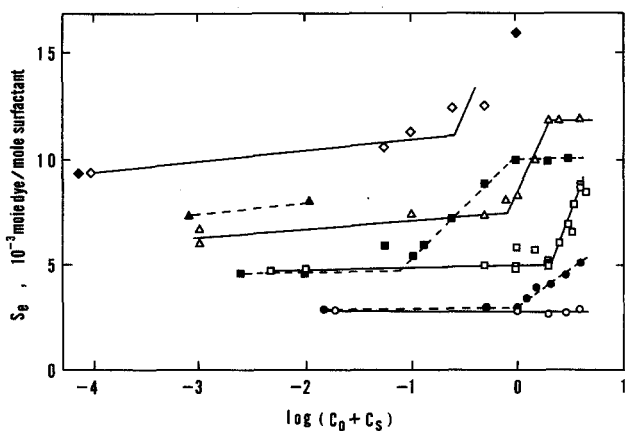


Fig. 5. Solubilization power of micellar surfactant toward Sudan Red B as a function of the logarithm of ionic strength. (○) DTAC at 25 °C, Ref. [12]; (●) DTAB at 25 °C, Ref. [12]; (□) TTAC at 25 °C; (■) TTAB at 25 °C; (△) CTAC at 25 °C; (▲) CTAB at 25 °C; (◇) STAC at 25 °C; (Φ) STAC at 35 °C; (◆) STAB at 35 °C

tant and is called the solubilization power:

$$S_e = S/(C - C_0). \quad (2)$$

The solubilization power of surfactant is independent of the micelle concentration at a given salt concentration, if the micelle size and shape are independent of micelle concentration.

The solubilization power of surfactant toward Sudan Red B is plotted against the logarithm of counterion concentration or of ionic strength, $\log(C_0 + C_s)$, in Figure 5, in which the data for DTAC in aqueous NaCl solution and DTAB in aqueous NaBr solution reported in the previous paper [12] are also included. The solubilization power of DTAC is almost constant at all ionic strengths. However, the solubilization power of DTAB and TTAC increases slightly and linearly with a logarithmic increase in ionic strength, and it increases abruptly but still linearly above a certain ionic strength. The solubilization power of TTAB and CTAC increases sharply above a certain ionic strength but becomes constant at further higher ionic strengths.

If the micelle aggregation number, m , is not influenced by the solubilization of dye, the solubilization capacity of a micelle, i. e., the average mole of solubilized dye per mole of micelle, is given by

$$\Sigma = m S_e. \quad (3)$$

In Figure 6, the values of solubilization capacity for TTAC, TTAB and CTAC micelles are plotted against

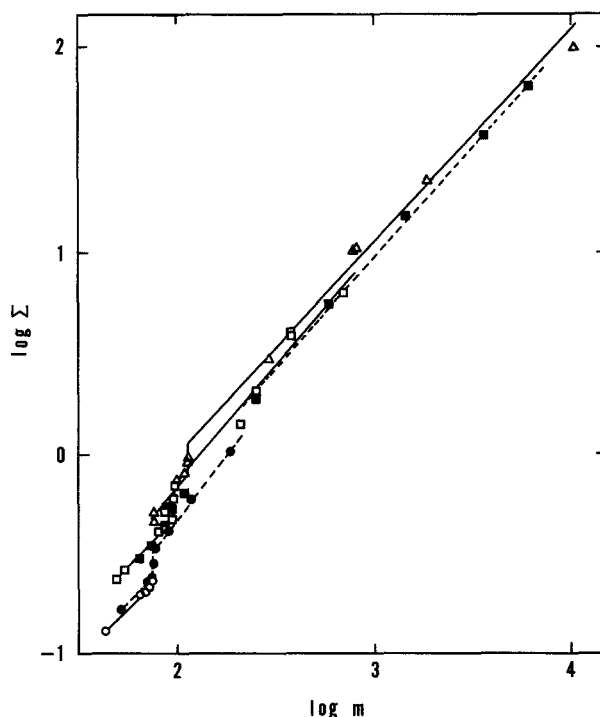


Fig. 6. Double logarithmic plot of solubilization capacity Σ of surfactant micelle toward Sudan Red B against the micelle aggregation number at 25 °C. (○) DTAC, Ref. [12]; (●) DTAB, Ref. [12]; (□) TTAC; (■) TTAB; (△) CTAC

the micelle aggregation number in the double logarithmic scale. The values of micelle aggregation number at given salt concentrations were taken from our recent work [14, 15] or derived therefrom. Data for DTAC and DTAB [12] are also included in Figure 6.

TTAC molecules in 3.0 M NaCl form rodlike micelles only above the micelle concentration of $0.58 \times 10^{-2} \text{ g cm}^{-3}$ (0.0199 M), which can be identified as the second critical micelle concentration [14]. Nevertheless, the plot of solubility vs. surfactant concentration in Figure 3 gives a straight line over the whole range of surfactant concentrations examined. The predominance of spherical micelles is the reason for this. Consequently, the aggregation number of the spherical micelle was chosen for the calculation of solubilization capacity of TTAC micelle in 3.0 M NaCl.

The solubilization capacity of DTAB, TTAC, TTAB, and CTAC micelles gradually increases with increasing micelle size and suddenly rises at a threshold value of aggregation number, m^* . At larger micelle sizes, the solubilization capacity gradually increases again.

Discussion

Solubilization properties of spherical micelles in water

Molecules of alkyltrimethylammonium halide in water form only spherical micelles above the critical micelle concentration [13–17]. The solubilization power and capacity values of spherical micelles in water are listed in Table 1. DTAC and DTAB [12] data are also included in Table 1. As seen in Figure 2(b), the solubilization power increases linearly with the number of carbon atoms in the alkyl chain, n_c , independent of counterion species, either chloride or bromide. The solubilization power increases by 2.16×10^{-3} mole dye/mole surfactant per addition of two CH_2 groups, and it follows that the relation holds for

$$S_e = 1.0_8 \times 10^{-3} n_c - 10.3 \times 10^{-3} \quad (4)$$

alkyltrimethylammonium micelles in water.

With an increase in the number of carbon atoms in the alkyl chain, the radius of a spherical micelle in water markedly increases [14]. Then the solubilization power increases with increasing alkyl chain length, since a micelle of surfactant with longer alkyl chain has a larger hydrophobic core. On the other hand, the solubilization power of DTAC in water is higher than that of dodecyldimethylammonium chloride (DDAC) [18]. The substitution of CH_3 for H on the polar head group reduces the radius of a micelle but markedly increases the surface area per surfactant ion [14]. The more bulky the polar head group, the less compact the packing of surfactant ions in the micelle; the solubilization is enhanced, in spite of the decrease in volume of the hydrophobic core. The packing of surfactant ions in a micelle is the same for chloride and bromide derivatives [12], and, therefore, the solubilization power in water is independent of the counterion species.

The solubilization capacity of spherical micelles in water increases with an increase in number of carbon atoms in the alkyl chain, and it is higher for bromide derivatives than for chloride derivatives, consistent with an increase in the volume of the hydrophobic core per micelle. The value of solubilization capacity is, however, lower than unity, even for spherical micelles of cetyltrimethylammonium ion (CTA^+).

Sphere-rod transition and solubilization

In micellar solutions some ionic surfactants form rodlike micelles as well as spherical micelles when the

salt concentration is higher than a certain threshold value [13–15, 17]. It is expected that the solubilization power of a surfactant and its dependence on the ionic strength will change with the structural transition of micelles from spherical to rodlike. Then the salt concentration above which the solubilization power markedly increases may be identified with the threshold salt concentration, C_s^* , for the sphere-rod transition of micelles.

The values of the threshold salt concentration obtained from the solubilization are summarized in Table 2. Values of the threshold salt concentration and the threshold aggregation number, m^* , obtained from light scattering measurements are also included there.

The sphere-rod transition occurs at a lower salt concentration, when the cationic surfactant has a longer alkyl chain and also its counterion is bromide rather than chloride, as shown in Figure 2(c). The logarithm of the threshold salt concentration changes linearly with the number of carbon atoms of alkyl chain. The relation is described by

$$\log C_s^* = -0.22_8 n_c + 3.5_7 \quad (5)$$

for the chloride derivatives and

$$\log C_s^* = -0.56_8 n_c + 6.9_5 \quad (6)$$

for the bromide derivatives. The effect of counterion species and alkyl chain length on the threshold salt concentration must be caused by different degrees of counterion binding. A micelle of surfactant with longer alkyl chain would bind a greater extent of counterions than one with a shorter alkyl chain, and Br^- would be bound on a cationic micelle to a greater extent than Cl^- . Consequently, a surfactant having a longer alkyl chain and with a bromide counterion will

Table 2. The threshold salt concentration and the threshold aggregation number for sphere-rod transition at 25°C

	C_s^*	m^*	
	(M) solu.	L.S. ^{a)}	L.S. ^{a)}
DTAC	no ^{b)}	no	—
DTAB	1.0 ^{b)}	1.8	80
TTAC	2.1	2.7	96
TTAB	0.08	0.12	98
CTAC	0.81	1.2	116
CTAB		0.06 ^{c)}	128 ^{c)}
STAC	~ 0.3		

^{a)} References [13–17]; ^{b)} Reference [12]; ^{c)} at 35°C

Table 3. Values of a and b in Equation (8), $S_e = a \log(C_o + C_s) + b$

	spherical		rodlike	
	a (10^{-3})	b (10^{-3})	a (10^{-3})	b (10^{-3})
DTAC ^{a)}	0.0	2.8		
DTAB ^{a)}	0.1	3.0	3.3	3.1
TTAC	0.2	5.1	11.3	1.5
TTAB	0.1	4.4	4.7	10.0
CTAC	0.4	7.5	11.2	8.6
CTAB	0.7	9.3		
STAC	0.6	11.6		

^{a)} Reference [12]

form rodlike micelles at a lower threshold salt concentration than a surfactant with a shorter chain and a chloride counterion. The threshold aggregation number ranges from 80 to 128 for C_{12} to C_{16} .

The linear relation of solubilization power with the ionic strength shown in Figure 5 can be represented by

$$S_e = a \log(C_o + C_s) + b. \quad (7)$$

The values of a and b are listed in Table 3. While the coefficient, a , for spherical micelles is very small for all surfactants, its value for rodlike micelles is 0.011 for two chloride derivatives and 0.004 for two bromide derivatives.

The solubilization capacity of micelles of alkyltrimethylammonium halides in aqueous salt solutions increases with increasing micelle size, but it abruptly rises around the aggregation number, m^* , of micelle formed at the threshold salt concentration of sphere-rod transition.

Solubilization properties of spherical and rodlike micelles in aqueous salt solutions

The molecular weights of spherical and rodlike micelles of an ionic surfactant generally increase as a salt is added to its aqueous solutions [13–15,17]. The solubilization power of a surfactant increases with an increase in ionic strength and thus with a growth of spherical and rodlike micelles.

As shown in Figure 6, the solubilization capacity depends on the micelle aggregation number but is independent of counterion species, either chloride or bromide. Sudan Red B can be solubilized more abundantly in rodlike micelles than in spherical micelles. For both spherical and rodlike micelles, the solubiliza-

Table 4. Values of α and β in Equation (9), $\log \Sigma = \alpha \log m + \beta$

	spherical		rodlike			
	α	β	α	β		
DTAC ^{a)}	1.0 ₄	-2.6 ₂	44 ≤ m < 76			
DTAB ^{a)}	1.0 ₈	-2.6 ₈	53 ≤ m < 76	1.3 ₂	-2.9 ₄	79 ≤ m
TTAC	1.0 ₆	-2.4 ₂	57 ≤ m < 95	1.1 ₄	-2.4 ₆	99 ≤ m
TTAB	0.9 ₅	-2.2 ₅	71 ≤ m < 96	1.1 ₀	-2.3 ₇	99 ≤ m
CTAC	1.2 ₈	-2.7 ₁	81 ≤ m < 111	1.0 ₄	-2.0 ₆	116 ≤ m

^{a)} Reference [12]

tion capacity is larger when the alkyl chain length is longer. It is realized that dyes are solubilized more readily in the larger hydrophobic core of micelle of surfactant with longer alkyl chain.

As seen in Figure 6, good linearity holds in both regions of spherical and rodlike micelles for each surfactant. The straight line can be represented by

$$\log \Sigma = \alpha \log m + \beta. \quad (8)$$

The values of α and β are summarized in Table 4. The coefficient, α , is nearly equal to unity for all surfactants, independent of the micelle shape. This means that the solubilization capacity is proportional to the micelle aggregation number, i. e., to the volume of spherical micelle or the contour length of rodlike micelle. The same results were reported for micelles of DDAC toward Sudan Red B [18] and of potassium soap toward ethylbenzene [4].

If the solubilization capacity is unity, one molecule of dye would be solubilized in a micelle. The aggregation number and contour length of rodlike micelles at $\Sigma = 1$ were obtained with reference to light scattering data [14, 15], and their values are shown in Table 5. The contour lengths were calculated, according to our procedure already reported [14]. With an increase in alkyl chain length, the aggregation number decreases from 169 for DTA^+ to 96 for CTA^+ , which corresponds to the change in contour length from 11.8 nm for DTA^+ to 5.3 nm for CTA^+ .

The solubilization power of TTAB and CTAC becomes constant at much higher ionic strengths, as seen in Figure 5. This indicates that long rodlike micelles can incorporate a definite number of dye molecules per surfactant, independent of their aggregation number or contour length. The values of its critical salt concentration, C_s^{**} , are given in Table 5. The values of aggregation number, m^{**} , and contour

Table 5. Aggregation number and contour length at $\Sigma = 1$, the critical salt concentration, aggregation number, and contour length for the constancy of solubilization power, and average contour length in a micelle per molecule of solubilized dye at 25 °C

	$m_{\Sigma = 1}$	$L_{c, \Sigma = 1}$ (nm)	C_s^{**} (M)	m^{**}	L_c^{**} (nm)	L_c/Σ (nm/molecule dye)
DTAB ^{a)}	169	11.8				
TTAC	144	9.2				7.5
TTAB	143	8.5	1.0	1480	88	5.7
CTAC	96	5.3	2.0	810	45	4.5

^{a)} Reference [12]

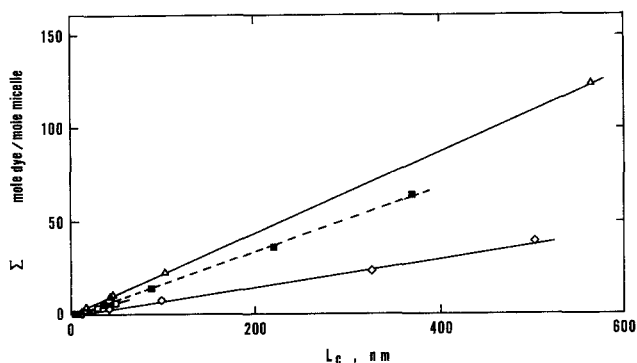


Fig. 7. Solubilization capacity Σ of surfactant micelle toward Sudan Red B against the contour length of rodlike micelle at 25 °C. (□) TTAC; (■) TTAB; (Δ) CTAC; (◇) DDAC

length, L_c^{**} , at the critical salt concentration were obtained according to the literature [14, 15] and are included in Table 5. They are about ten times larger than the values of the aggregation number and contour length at $\Sigma = 1$. The constancy of solubilization power was also obtained for DDAC at the critical NaCl con-

centration of 1.5 M, where the aggregation number and contour length were 585 and 38 nm, respectively [12, 14].

The solubilization capacity of rodlike micelles of TTAC, TTAB, and CTAC is plotted in Figure 7 against the contour length of micelle, which was calculated from the micelle molecular weight, as described in the previous paper [14, 15]. The solubilization capacity linearly increases with an increase in contour length. The length of rodlike micelle per molecule of solubilized dye, L_c/Σ , in which one molecule of Sudan Red B is solubilized, is obtained from the slope of a straight line in Figure 7, and the values are included in Table 5. They range from 4.5 nm for CTAC to 7.5 nm for TTAC and are close to the contour length at $\Sigma = 1$. The same plot for the solubilization capacity of DDAC [18] leads to the result that one molecule of Sudan Red B can be solubilized per 14 nm of rodlike micelle of DDAC. The smaller L_c/Σ value for a rodlike micelle of surfactant having a longer alkyl chain and more bulky head group can be attributed to the larger hydrophobic core of the micelle and the less

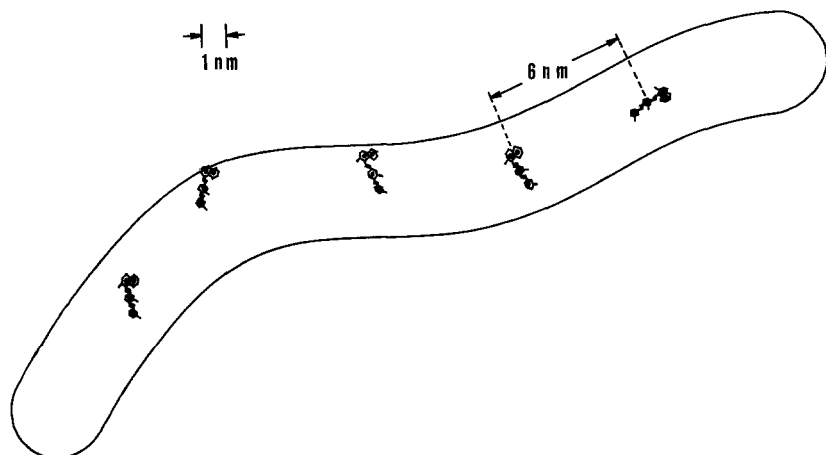


Fig. 8. Schematic profile of solubilized Sudan Red B molecules in a rodlike micelle of TTAB in 0.5 M NaBr at 25 °C

compact packing of surfactant ions in a micelle, respectively.

A molecule of Sudan Red B is about 1.8 nm in length. TTAB forms rodlike micelles in 0.5 M NaBr, the contour length of which is 38.6 nm [14]. Five dye molecules, then, will be inserted into the rodlike micelle in a manner as schematically presented in Figure 8. There a molecule of nonpolar Sudan Red B will be situated in the hydrophobic interior of a rodlike micelle rather than near its polar surface [18].

Acknowledgement

We thank Mrs. Hiroko Kotani for her help with the gas chromatographic measurement.

References

1. Hartley GS (1938) *J Chem Soc* 1968
2. McBain JW, Johnson KE (1944) *J Am Chem Soc* 66:9
3. McBain JW, Green AA (1946) *J Am Chem Soc* 68:1731
4. Stearns RS, Oppenheimer H, Simon E, Harkins WD (1947) *J Chem Phys* 15:496
5. Moroi Y, Sato K, Matuura R (1982) *J Phys Chem* 86:2463
6. Rosen MJ (ed) (1978) *Surfactants and Interfacial Phenomena* 125, John Wiley & Sons, New York
7. Kolthoff IM, Stricks W (1948) *J Phys Coll Chem* 52:915
8. Brown JB, Nauman RV (1967) *J Coll Interf Sci* 23:302
9. Robins DC, Thomas IL (1968) *J Coll Interf Sci* 26:422
10. Tokiwa F (1968) *J Phys Chem* 72:1214
11. Jacobs PT, Geer RD, Anacker EW (1972) *J Coll Interf Sci* 39:611
12. Imae T, Abe A, Taguchi Y, Ikeda S (1986) *J Coll Interf Sci* 109:567
13. Imae T, Kamiya R, Ikeda S (1985) *J Coll Interf Sci* 108:215
14. Imae T, Ikeda S (1986) *J Phys Chem* 90:5216
15. Imae T, Ikeda S, submitted
16. Ozeki S, Ikeda S (1981) *Bull Chem Soc Japan* 54:552
17. Ozeki S, Ikeda S (1982) *J Coll Interf Sci* 87:424
18. Ozeki S, Ikeda S (1985) *J Phys Chem* 89:5088

Received November 25, 1986;
accepted February 20, 1987

Authors' address:

Dr. Toyoko Imae
Department of Chemistry
Faculty of Science
Nagoya University
Chikusa-ku, Nagoya 464, Japan